Cement and Concrete Research 38 (2008) 1401–1408

Contents lists available at ScienceDirect

Cement and Concrete Research

journal homepage: http://ees.elsevier.com/CEMCON/default.asp

Capillary suction and diffusion model for chloride ingress into concrete

David Conciatori *, Hamid Sadouki, Eugen Brühwiler

EPFL-MCS, Swiss Federal Institute of Technology (EPFL), Lausanne, Switzerland

ARTICLE INFO

Article history:
Received 19 March 2007
Accepted 26 June 2008

Keywords:
Concrete transport capillary water model

ABSTRACT

A numerical approach, named TransChlor, is proposed to simulate transport phenomena of various substances in concrete. This approach is a theoretical model based on finite elements and finite differences methods. The model consists of coupled nonlinear partial differential equations based on Fick's diffusion law and on kinematics equations. Simulation results from a parametrical study highlight the influence of microclimatic conditions, exposure to deicing salts and concrete cover permeability and thickness on chloride ingress in concrete. The results show that the chloride ion concentration increases quickly in concrete cover when a structure is exposed to deicing salts at a mountainous location; whereas permeability of concrete cover is an insignificant parameter when the concrete is in direct or splash water contact.

1. Introduction

The corrosion initiation period [6] includes the time during which substances such as water, chloride ions and carbon dioxide flow through the concrete cover (i.e. the clear concrete cover protecting the steel reinforcement) and reach the certain concentration necessary to trigger corrosion of the steel reinforcement. The initiation period is characterized by chemical reactions between the various substances and the movement of the various substances in the concrete.

Two models are used, each taking into account a different scale: microscopic and macroscopic models. Microscopic models consider the flow of ions and their chemical balance in the concrete, such as the models Stadium [15], Ms Diff [29], Masi [16], by Shin [27] and Schmidt-Döhl [25,26]. Macroscopic models take into account the various thermal variation as well as hydrous and ionic movements. The chemical reactions are considered only through parameters simulating the chemical effects on transport, like the models by Roelfstra [21], TransChlor [6], ClincConc [28], by Meijers [17], Saetta [22] and Ishida [10,14]. While microscopic models simulate the phase changes more precisely and take into account the porosity reduction, they often require extensive testing to obtain valid data for the model parameters.

The TransChlor model is an original model to address chloride ion movement with water in concrete and to consider microclimates [4,5] reconstituted from real climates. The data is taken from meteorological stations and is reconstituted by considering exposure level of a reinforced concrete structural element. The water movement is accelerated in situations when their adhesion forces between the water and the porous structure of concrete contribute to this movement. This phenomenon is known as capillary suction. The vapour movement is less sensitive to capillarity suction. Instead it follows a diffusion process. Transport of water and water vapour is differentiated in the model [2,21,23]. The water transport parameters are obtained from laboratory tests on water adsorption at low temperatures [6,7].

The TransChlor model basically uses the Fick's diffusion law for water vapour transport [3,18], thermal diffusion and chloride ion diffusion in water [6]. This law allows the simulation of the diffusion process due to a concentration gradient of these substances. Although the Fick's diffusion law represents vapour diffusion well, it does not describe capillary suction of water as observed in own laboratory tests [6] and by other researchers [11,21,24]. Accurate capillary suction modelling is thus obtained by considering the kinetics of the phenomenon.

2. Transport model

The chloride ion transport in concrete cover is modelled with TransChlor. The relevant parameters considered are the microclimate, the presence of deicing salts and the concrete cover permeability of the structural element. The microclimate is a function of the structural element's exposure to solar radiation (zones in the shade are distinguished from those exposed to the sun), the annual average carbon dioxide concentration and the geographically linked weather conditions (air temperature, relative humidity and precipitation) [6].

The TransChlor model considers the thermal diffusion process and the hydrous transport by capillarity suction and vapour diffusion as a function of the carbonation state, while simulating chloride ion transport in concrete [4,6,8]. The various transport processes are modelled with Fick's Eqs. (1)–(3). The model uses the finite element method to solve for the ion propagation within the concrete and the finite differences method (an implicit method) to solve for the duration of progression of the propagation front.

* Corresponding author. Laval University, Pavillon Adrien-Pouliot, local 2928G, Québec, Canada G1K 7P4.
E-mail address: david.conciatori@gci.ulaval.ca (D. Conciatori).

0008-8846/$ – see front matter © 2008 Elsevier Ltd. All rights reserved.
doi:10.1016/j.cemconres.2008.06.006

Eq. (1) describes the thermal diffusion process. The specific heat capacity, c_T, depends on moisture content, w, while the thermal conductivity, λ_T, is a function of moisture content, w, and temperature, T [9].

In Eq. (2) hydrous transport is modelled by vapour diffusion, D_h, and water capillary, D_{cap}, coefficients. Vapour transport is a function of the temperature, T, and the moisture content, w [3]. The temperature effect is described by means of the Arrhenius law. Water transport is a function of the concrete temperature, T, the moisture content, w, the pore humidity, h_r, and the duration of contact of concrete with water, $t_{contact}$.

The carbon dioxide, CO_2, transport governs the carbonation progression in concrete. The extent of carbonated concrete is required to determine the amount of chloride ions absorbed by the cement paste. Concrete carbonation depth, x_c, expressed by Eq. (3) is obtained by considering the moisture content, the concrete permeability to CO_2 and the chemical carbonation reaction rate [19]. The external conditions are represented by the molar carbon dioxide concentration $[CO_2]$. The carbonation reaction rate is described by the molar concentrations of calcium hydroxide $[Ca(OH)_2]$ and calcium silicate hydrate [CSH]. The concrete carbon dioxide diffusion coefficient, $D_{e,CO2}$, takes into account the concrete permeability and the moisture content evolution in the concrete pores.

$$\frac{\partial T}{\partial t} = \mathrm{div}\left(\frac{\lambda_T(T,w)}{c_T(w)} \cdot \overrightarrow{\mathrm{grad}(T)}\right) \tag{1}$$

$$\frac{\partial h_r}{\partial t} = \mathrm{div}\left(D_h(T,h_r) \cdot \overrightarrow{\mathrm{grad}(h_r)}\right) - \overrightarrow{D_{cap}}(t_{contact}, h_r, E/C, T) \circ \overrightarrow{grad(h_r)} \tag{2}$$

$$x_c = \sqrt{\frac{2 \cdot [CO_2] \cdot D_{e,CO2}}{[Ca(OH)_2] + 3 \cdot [CSH]}} \cdot \sqrt{t} \tag{3}$$

The transport of chloride ions following Eq. (4) is a function of the chloride ion diffusion through the pore water defined by moisture content, w, and the movement of entrained chloride ions desolved in water moving through the concrete described by Eq. (2) [6]. This phenomenon is referred to as convection. The retardation of the chloride ion front with respect to the convection induced water movement is taken into account by including the retardation coefficient, R_{Cl}. Hardening cement paste and the carbonation rate trap a certain amount of chloride ions [13,20,28]. The chloride ions bound in the cement paste, c_b, are distinguished from the free chloride ions moving through the concrete, c_f. The relation between total amount of chloride ions C, c_f and c_b is given by Eq. (5), including the Freundlich isotherm with constant parameters β and γ. Chloride ion diffusion coefficient in water, D_{Cl}, varies with the temperature following the Arrhenius law [30].

$$\frac{\partial C}{\partial t} = \mathrm{div}\left(R_{Cl} \cdot c_f \cdot D_h \cdot \overrightarrow{\mathrm{grad}(h_r)} + w(h_r,T) \cdot D_{Cl} \cdot \overrightarrow{\mathrm{grad}(C)}\right) + R_{Cl} \cdot c_f \cdot \left(\overrightarrow{D_{cap}} \circ \overrightarrow{\mathrm{grad}(h_r)}\right) \tag{4}$$

$$C = c_f \cdot w + c_f^{\beta} \cdot \gamma \tag{5}$$

3. Chloride ion transport by water

The mean velocity or the flow of water is discretised by the finite element method. The positive or negative sign in Eq. (6) depends on the direction of water flow.

$$\overrightarrow{q} = D_h \cdot \overrightarrow{\mathrm{grad}(h_r)} \pm \overrightarrow{D_{cap}} \cdot h_r \tag{6}$$

D_{cap} [mm/s] capillarity coefficient
D_h [mm^2/s] water vapour diffusion coefficient
H [−] relative humidity in the concrete pores
$\overrightarrow{q}$ [mm/s] water flow or speed

The weak form can be written as Eq. (7).

$$q = \int_{h_L}^{h_R} D_h \cdot [N(x)]^T \cdot [B(x)] \cdot dh \pm D_{cap} \cdot [I] = \frac{D_h}{2} \cdot \begin{bmatrix} -1 & 1 \\ -1 & 1 \end{bmatrix} \cdot \begin{Bmatrix} h_1 \\ h_2 \end{Bmatrix} \pm D_{cap} \cdot \begin{bmatrix} 1 & 0 \\ 0 & 1 \end{bmatrix} \cdot \begin{Bmatrix} 1 \\ 1 \end{Bmatrix} \tag{7}$$

$[N(x)]$ interpolation matrix function
$[B(x)]$ matrix of relation for flow and concentration of h
$[I]$ identity matrix
x location in the concrete
h relative humidity at the node

The assembly of all the elements allows calculating the water flow velocity at each node, Eq. (8).

$$\begin{Bmatrix} q_0 \\ q_1 \\ q_2 \\ \dots \\ q_n \end{Bmatrix} = \frac{1}{2} \cdot \begin{bmatrix} -D_{h0} & D_{h0} & 0 & \dots & 0 \\ -D_{h0} & D_{h0}-D_{h1} & D_{h1} & \dots & 0 \\ 0 & -D_{h1} & D_{h1}-D_{h2} & \dots & 0 \\ \dots & \dots & \dots & \dots & D_{h,n-1} \\ 0 & 0 & 0 & -D_{h,n-1} & D_{hn} \end{bmatrix} \cdot \begin{Bmatrix} h_0 \\ h_1 \\ h_2 \\ \dots \\ h_n \end{Bmatrix} \pm \begin{bmatrix} D_{cap0} & 0 & \dots & 0 \\ 0 & D_{cap1} & \dots & 0 \\ \dots & \dots & \dots & 0 \\ 0 & 0 & 0 & D_{capn} \end{bmatrix} \cdot \begin{Bmatrix} 1 \\ 1 \\ 1 \\ \dots \\ 1 \end{Bmatrix} \tag{8}$$

The average movement of the chloride ions takes into account on each node the delay coefficient and the considered time interval, according to Eq. (9).

$$d_{Cl,i} = q_i \cdot R_{Cl} \cdot \Delta t \tag{9}$$

d_{Cl} [mm] average movement of the chloride ions
R_{Cl} delay coefficient
Δt [s] time interval
i node number

Fig. 1a shows that the chloride ion concentration assessment is distorted by using a conventional method [21]. Eq. (10) provides the algorithm taking into account chloride ion conservation.

$$\begin{Bmatrix} B_0 \\ B_1 \\ B_2 \\ \dots \\ B_n \end{Bmatrix} = \frac{1}{8} \cdot \begin{bmatrix} 3 \cdot l_0 & l_0 & 0 & \dots & 0 \\ l_0 & 3 \cdot (l_0 + l_1) & l_1 & \dots & 0 \\ 0 & l_1 & 3 \cdot (l_1 + l_2) & \dots & 0 \\ \dots & \dots & \dots & \dots & l_{n-1} \\ 0 & 0 & 0 & l_{n-1} & 3 \cdot l_{n-1} \end{bmatrix} \cdot \begin{Bmatrix} c_{f0} \\ c_{f1} \\ c_{f2} \\ \dots \\ c_{fn} \end{Bmatrix} \tag{10}$$

B [kg mm/m^3] surface connecting the chloride ion concentration to the dimension of the finite element
l [mm] finite element length
c_{fi} [kg/m^3] free chloride ion concentration at the ith node, related to the liquid solution

Each surface, B_i, is assigned to the node of displacement vector (Fig. 1b) and undergoes a displacement d_i. The surface, B_i, is not inevitably on a node after this displacement. This surface is assigned on the nodes by using the static resolution analogy of a simple beam to take into account the influence of the element distance. As illustrated in Fig. 2, the surface, B_i, will be assigned

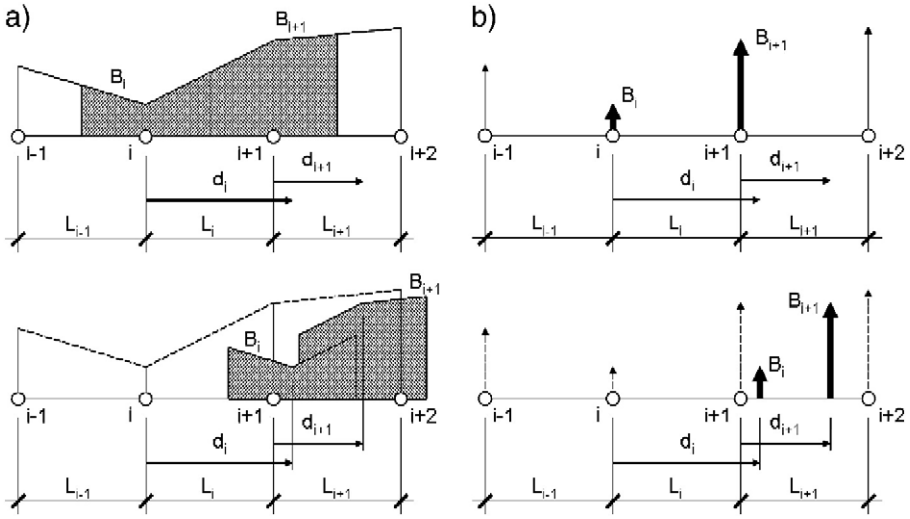

Fig. 1. Chloride ion movement: a) inconsistency due to surface superposition, b) transformation on the surface represented by a vector assigned to a node.

on the node $i+1$ and $i+2$ with Eqs. (11) and (12) for the example developed in Fig. 1.

$$D_{i+1} = \frac{B_i \cdot b}{l_{i+1}} \tag{11}$$

$$D_{i+2} = \frac{B_i \cdot a}{l_{i+1}} \tag{12}$$

D [kg mm/m^3] surface relating the chloride ion concentration to a distance represented by the finite element dimensions

a and b [mm] vector position distances B_i according to the simple beam analogy

Finally, the chloride ion concentration is obtained starting from an identical equation to Eq. (10), but with the unknown being the vector of the chloride ion concentrations, illustrated as Eq. (13).

$$\begin{Bmatrix} D_0 \\ D_1 \\ D_2 \\ \dots \\ D_n \end{Bmatrix} = \frac{1}{8} \cdot \begin{bmatrix} 3 \cdot l_0 & l_0 & 0 & \dots & 0 \\ l_0 & 3 \cdot (l_0 + l_1) & l_1 & \dots & 0 \\ 0 & l_1 & 3 \cdot (l_1 + l_2) & \dots & 0 \\ \dots & \dots & \dots & \dots & l_{n-1} \\ 0 & 0 & 0 & l_{n-1} & 3 \cdot l_{n-1} \end{bmatrix} \cdot \begin{Bmatrix} c_{f0} \\ c_{f1} \\ c_{f2} \\ \dots \\ c_{fn} \end{Bmatrix} \tag{13}$$

Local equilibrium [1] on the nodes at the extremities is not guaranteed. However, the boundary condition values of the chloride ion concentration in water are assigned to these nodes.

4. Validation

Comparison of measured temperatures of laboratory samples and the TransChlor results validate the thermal transfer simulation model. The sample temperatures are between 20 °C and −20 °C [6,7].

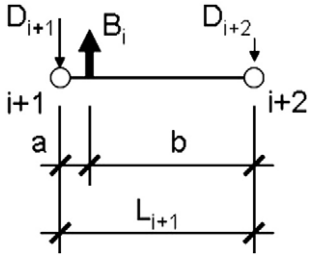

Fig. 2. Simple beam analogy for assigning surfaces B_i to the node.

The TransChlor model also simulates transfer by means of capillary suction [6]. The model reproduces the chloride ingress due to convection by water well. To validate the modelled water transport, lab test on an immersed sample in brine at low temperatures is performed [7]. The chloride and water front passage are determined experimentally and numerically in a concrete sample with water to cement ratio of 0.52. In the experiment the sample is subjected to the capillary test. A chloride sensor consisting of an optical fibre placed in the concrete sample at 18 mm from the surface measures the chloride concentration. The results of the measurements and simulations are variable for the first 8 days of the exposure period and become identical thereafter [12].

5. Parametric study

5.1. Definition of parameters

Deicing salts are spread on roadways in winter periods. As a result, chloride ions come into contact with concrete structural elements through salt-laden mist (water vapour), and the saline water that is either in direct and permanent contact with the elements or splashed on them by passing vehicles.

The relevant variables analysed are the microclimate, the presence and concentration of deicing salts, the properties of the concrete cover and the carbonation depth (Table 1):

- The microclimate depends on the geographical location and takes into account air temperature, air relative humidity and precipitation. The corresponding data have been obtained from three

Table 1
Parameters investigated using the TransChlor model

Parameters	Parameter variation
Spreading type	Mechanical spreading, automatic spreading
Types of exposure	Stagnant water, splash water, mist
Concrete permeability	Concrete A, Concrete B, Concrete C
Geographical location	Zurich-Kloten, Pully, Davos
Concrete cover thickness	15 mm, 30 mm, 60 mm

Table 2
Swiss areas with altitudes of each location (A: altitude, T: average annual air temperature, RH: average annual air relative humidity)

Areas (location)	A [meters above sea level]	T [°C]	RH [%]
Mountainous (Davos)	1590	2.8	73.2
Lake Geneva (Pully)	461	10.4	71.7
Swiss Plateau (Zurich-Kloten)	436	8.5	77.6

different meteorological stations in Switzerland: the mountainous area in Davos, the Swiss Plateau in Zurich-Kloten and the Lake of Geneva area at Pully.
- The elements are exposed to stagnant water, splash water and mist.
- The concentration of deicing salts evolves in time depending on the application rate and the local weather conditions for a given geographical location. The chloride ion concentration depends primarily on the type of salt spreader, i.e., mechanical spreading (of either solid salt or brine) or automatic spreading (of brine).

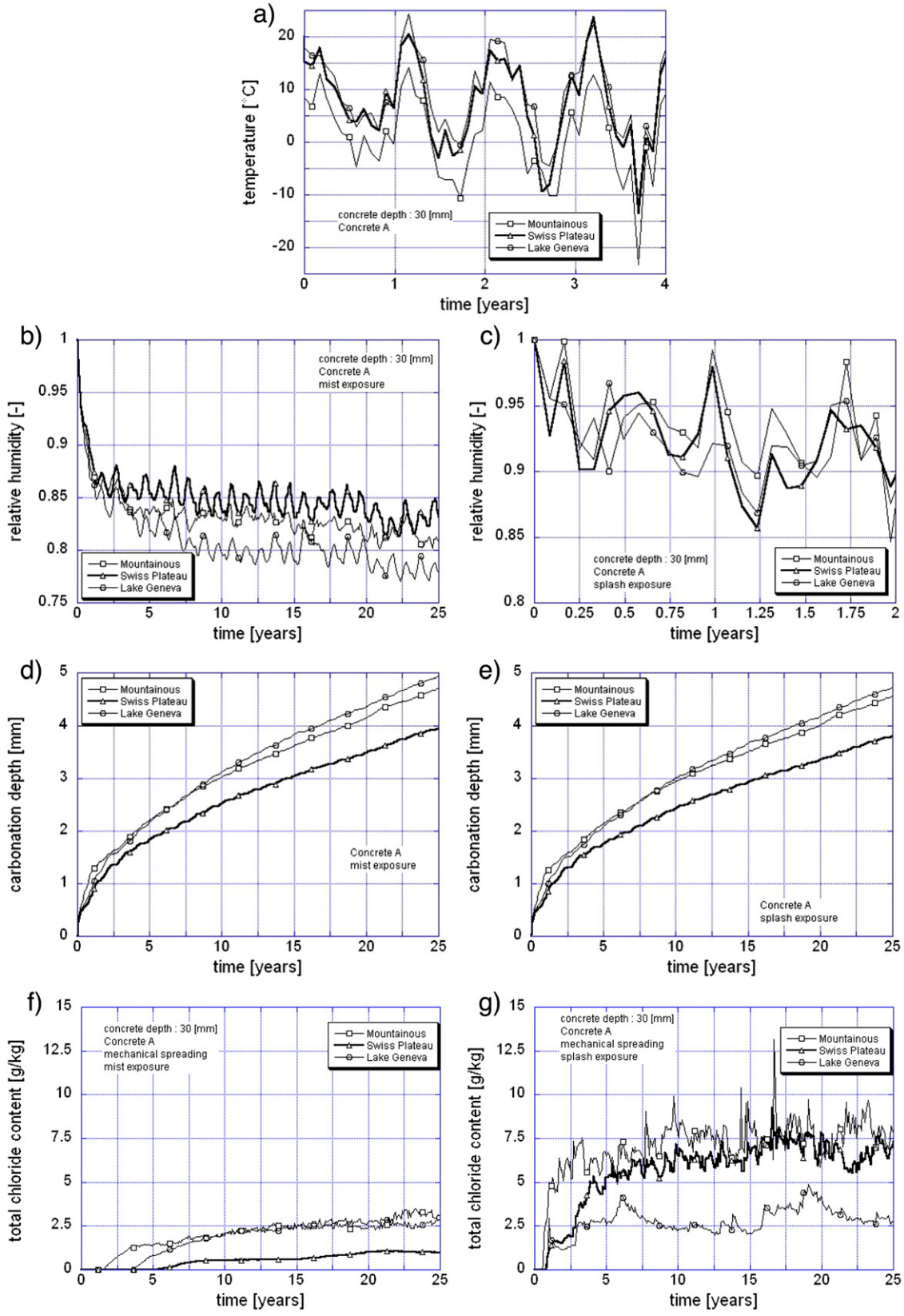

Fig. 3. Influence of geographical location on chloride ion transport as simulated with TransChlor.

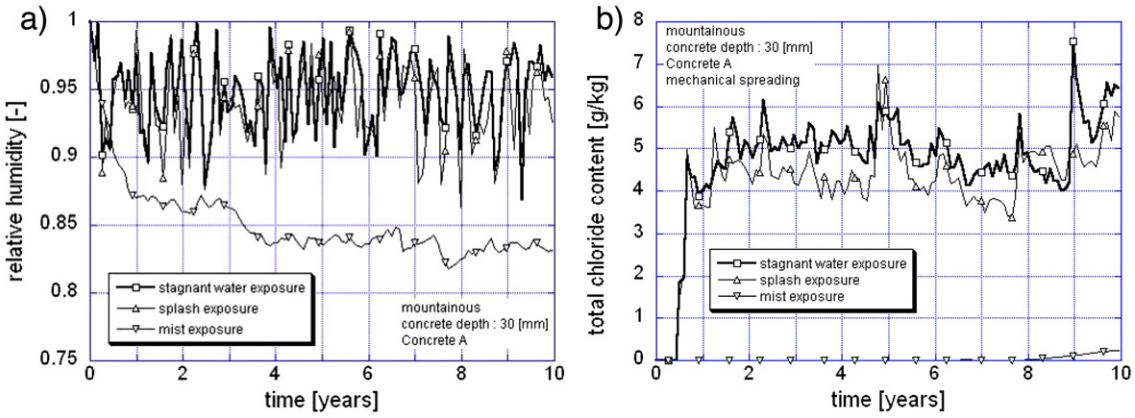

Fig. 4. Influence of structural element exposure as simulated with TransChlor on a) relative humidity of concrete and b) total chloride content.

- The permeability and thickness of the concrete cover and the corrosion resistance of the reinforcing steel influence the resistance of the structural element. Three different concrete cover permeabilities are chosen: low permeability Concrete A, average permeability Concrete B and high permeability Concrete C. The effect of concrete cover thickness is investigated for three different values of 15, 30 and 40 mm.

The chloride ingress is much slower under mist exposure than under stagnant or splash water exposure. Therefore, the evolution of chloride ion content in the concrete is simulated over 25 years for elements exposed to stagnant or splash water, and over 50 years for concrete elements subjected to mist exposure.

5.2. Geographical location

Chloride ions migrate rapidly into the concrete cover during precipitation periods with and without the presence of deicing salt. Seasonal variations can significantly influence chloride ion profiles (i.e., chloride ion concentration as a function of concrete depth). Due to the significant chloride ion transport towards larger depth in the concrete, chloride ion profiles may show significant concentrations at the steel reinforcement level during winter periods and reduced concentrations in summer. The space variability of the moisture content develops differently depending on the type of contact with water (exposure to stagnant or splash water) or water vapour (mist exposure). This has a direct impact on the chloride ion convection by water.

Table 2 shows that the temperature decreases with increasing altitude of the location [6]. The lowest temperatures are recorded in the mountainous area, while the temperatures in the plains are moderate (Fig. 3a).

The air relative humidity is reflected directly by the relative humidity in the concrete pores for mist exposure. Initial condition considers a completely saturated concrete. The Swiss Plateau is the wettest climate, followed by the mountainous and the Lake of Geneva areas, respectively (Fig. 3b). The relative humidity in the concrete pores is directly related to the precipitations in a given area and class of exposure as shown in particular for splash exposure. Fig. 3c shows the fluctuations and the high values of relative humidity in concrete pores for the mountainous area due to the significant precipitations in the region.

In Fig. 3d and e, the simulation results for splash and mist exposure zones illustrate that for low moisture level the rate of concrete carbonation is faster. As shown in the figures, the rate of carbonation is slowest for the Swiss Plateau, where the air relative humidity is higher than for the Lake of Geneva and mountainous areas for which the rate of carbonation of concrete are similar.

Under mist exposure, chloride ion ingress is similar for all three areas (Fig. 3f). This evolution is explained by the similar relative humidity level in each location. The chloride ion diffusion becomes important and is similar for each location.

The evolution of chloride ion ingress under splash exposure is fastest in mountainous areas (Fig. 3g). For the Swiss Plateau, this evolution is slow in the initial stage, but its rate increases. In about 10 years it reaches values close to the ones for the mountainous area, and after it remains constant. The chloride ion concentration evolution remains rather slow for the Lake of Geneva area because the amount of deicing salt spread on the road is less than the other areas.

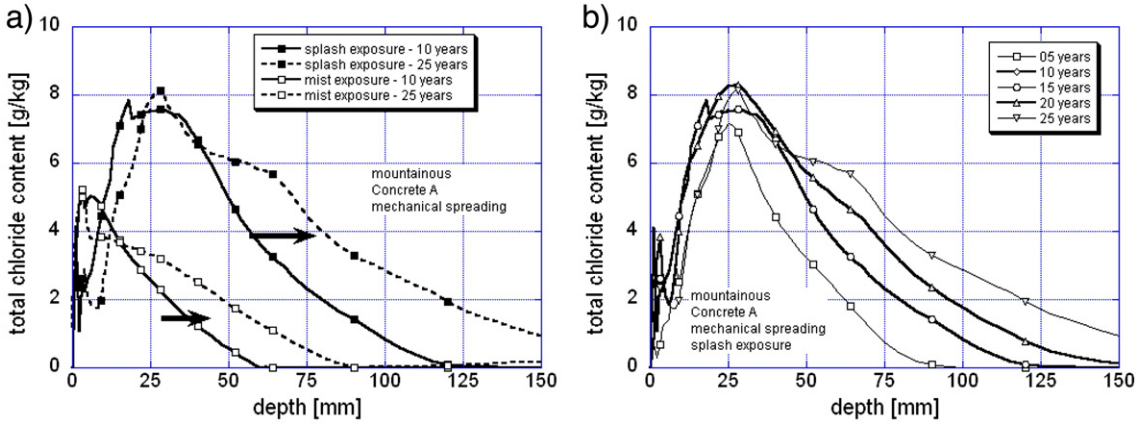

Fig. 5. Spatial variation of the total chloride content in concrete for different a) type of exposure and b) time of exposure.

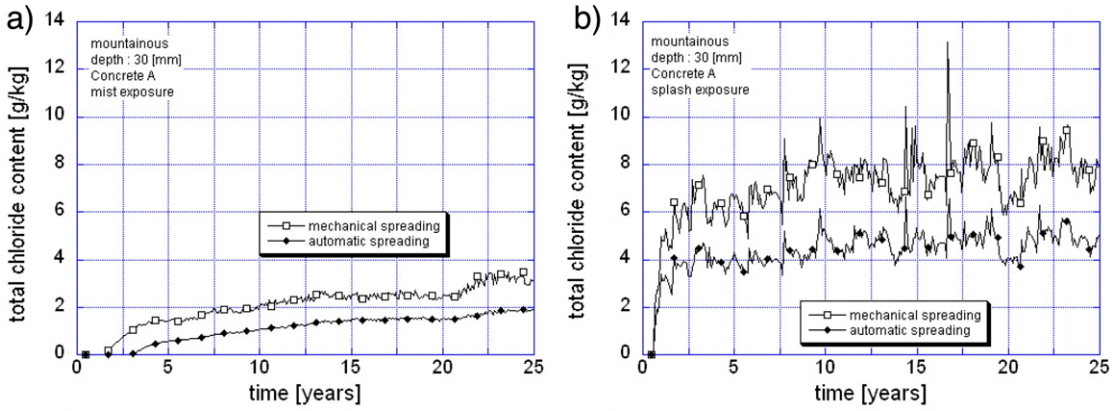

Fig. 6. Influence of spreading type on chloride ion concentration for a) mist and b) splash exposure.

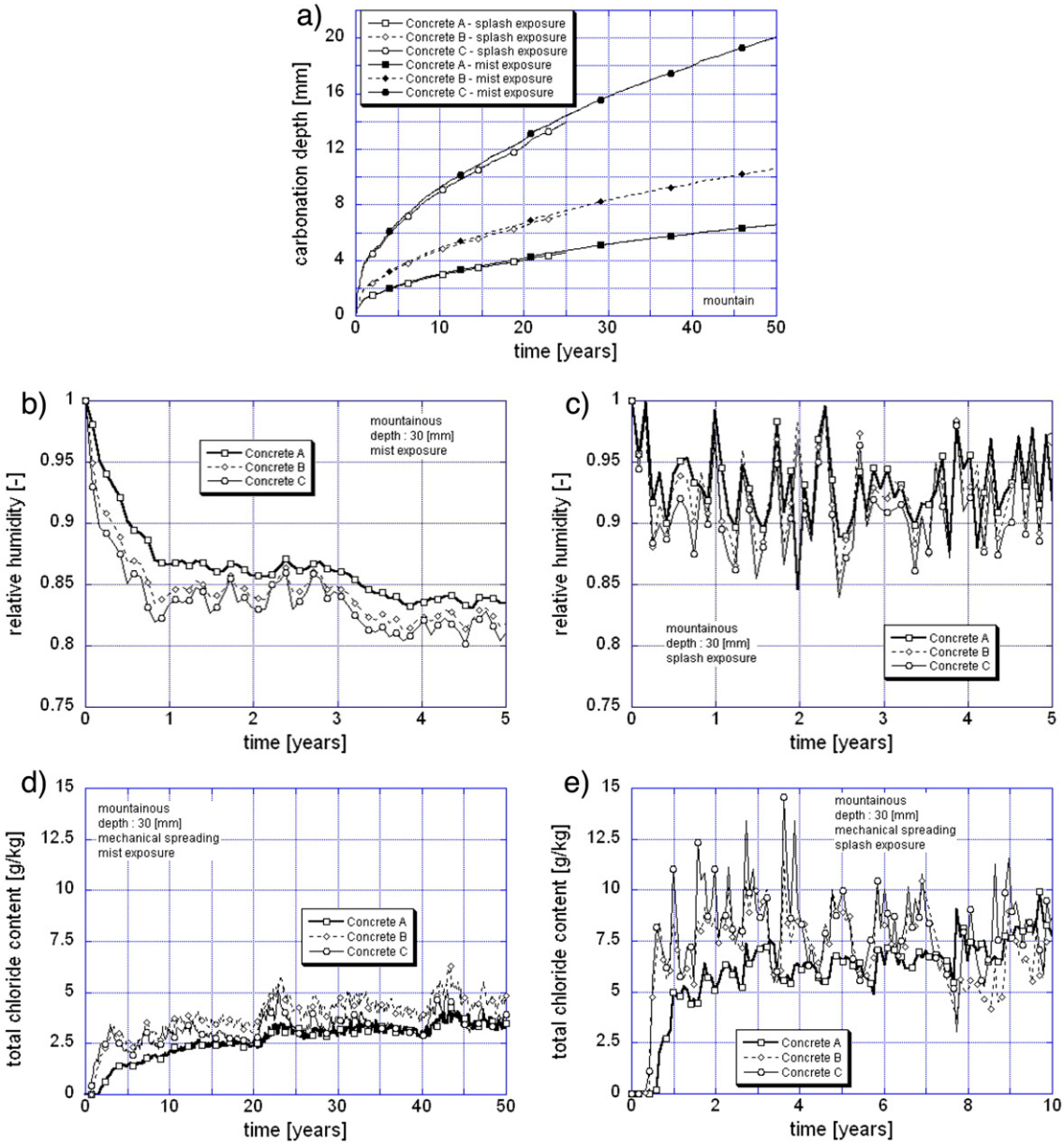

Fig. 7. Influence of concrete permeability on the various transport modes as simulated with TransChlor.

5.3. Exposure of the structural element

The presence of water on a structural element is taken into account by stagnant water and splash exposure. The stagnant water and splash exposure zones have a similar evolution of relative humidity while mist exposure has a smaller fluctuation in relative humidity (Fig. 4a). The relative humidity under mist exposure remains constant at about 83% after 10 years, which is about 10% higher than the average annual air relative humidity.

Chloride ion ingress into concrete cover is much more significant for the stagnant water and splash exposures than for mist exposure (Fig. 4b). Furthermore, the chloride ion evolutions for former two cases are similar. The contact time of the structure with water is not different for these two exposures. This contact time comprises a large variability for the stagnant water exposure and is directly related to the drying time of water trapped in the concrete near the surface.

Fig. 5a demonstrates that a significantly larger amount of chloride ions migrate into concrete under splash exposure than under mist exposure. Maximum chloride ion concentration occurs at a depth away from the surface. The concentration of chloride ions at the concrete surface is rather low. This is due to the transport of the ions by the capillary suction. Fig. 5b shows that the chloride profile after 5 years is similar to the one after 25 years; thus, the maximum chloride ion concentration is reached after 5 years. With time chloride ions only migrate further into the concrete but chloride ion concentration does not increase.

5.4. Type of deicing salt spreading

The amount of deicing salt spread on the roadway depends on the chosen spreading type, i.e., the mechanical or automatic spreading. Typical amounts of salt spread in a mountainous area for mechanical and automatic spreading are 1497 and 1213 [g/m^2 year], respectively [6].

The chloride ion evolution in concrete is slower in the case of automatic spreading (Fig. 6). For mist exposure after 50 years, the

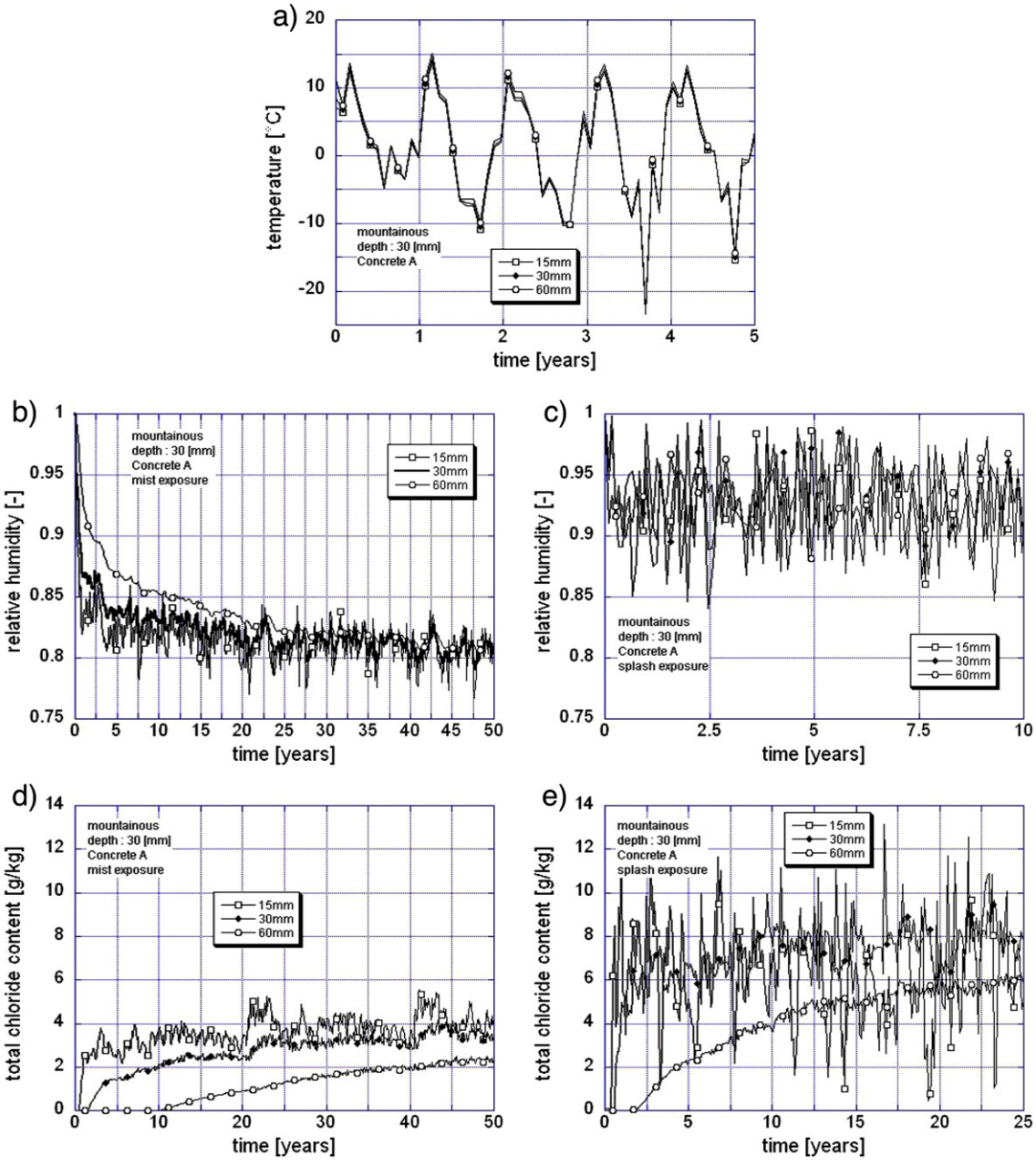

Fig. 8. Influence of concrete thickness on the various transport modes as simulated with TransChlor.

chloride ion concentration amounts to approximately 45% of that calculated for mechanical spreading.

5.5. Concrete permeability

Movements of substances in concrete depend directly on the concrete permeability for all transport modes, except for the thermal transfer. Fig. 7 shows that the ingress of chloride ions, propagation of carbonation and evolution of relative humidity is most significant for Concrete C with the highest permeability.

The pores filling rate is illustrated for two different types of exposure: splash water and mist exposure. The wetting and drying fluctuations are faster in the Concrete C for zones expose to splash water (Fig. 7b and c).

In comparison to Concrete C, the carbonation depth is reduced to about one third for Concrete A and to one half for Concrete B (Fig. 7a). The results in Fig. 7 also indicate that there is only a small influence of permeability on the chloride ion concentration. In fact, after 10 years of splash exposure, the chloride content is the same for all three types of concretes.

The results of chloride concentrations from the simulations are frequently observed in structural elements exposed to deicing salts due to splash exposure for more than 20 years, when they show significant signs of corrosion requiring rehabilitation.

5.6. Concrete cover thickness

The concrete temperature changes very quickly with the external environment. Therefore, instead of a thermal diffusion model for predicting the change of the temperature in the concrete cover, the meteorological temperature data with a time step of more than 1 h can be used (Fig. 8a). The hydrous transfer attenuates the relative humidity gradients in the concrete depth. This attenuation is more important for thicker members under mist exposure (Fig. 8b and c). The chloride ion evolution in the concrete cover is particularly important in the case of splash exposure. Depths of more than 60 mm show an already important attenuation of the chloride concentrations at 25 years. The rate of chloride ion evolution in the concrete, however, remains slow for a salt-laden mist exposure (Fig. 8d and e).

6. Conclusions

Water movement by capillary suction is modelled with kinematic equations. This movement is transformed into chloride ion movement due to the chloride ion convection in water. This phenomenon is implemented in the TransChlor Model to simulate chloride ingress into concrete cover. The model also considers reconstituted microclimatic conditions. The following conclusions can be drawn from the TransChlor numerical simulations:

1. Chloride ion concentration increases quickly in the concrete cover when structural elements are exposed to deicing salts and water (splash and direct contact).
2. Maximum chloride content is reached after less than 10 years at a depth of about 20 to 40 mm from the surface.
3. Chloride ingress significantly depends on the climatic condition and the amount of deicing salts applied. Permeability of concrete cover is thus a rather insignificant parameter when the concrete is in direct and splash water contact.

References

[1] A. Andersen, Investigation of chloride penetration into bridge columns exposed to deicing salt, HETEK-report No.82, Danish Road Directorate, Copenhagen, 37pp., 1997.
[2] V. Baroghel-Bouny, Caractérisation des pâtes de ciment et des bétons, LCPC et ministère de l'équipement des transports et du tourisme, 468, Paris, France, 1994.
[3] Z. Bazant, Creep and shrinkage of concrete: mathematical modelling, Materials and Structures 20 (5) (September 1987).
[4] D. Conciatori, E. Denarié, E. Brühwiler, Influence of microclimate on the probability of initiation of chloride induced corrosion in reinforced concrete, in: P. Schiessl (Ed.), 4th International Ph.D. Symposium in Civil Engineering, Springer-VDI, Munich Germany, September 2002.
[5] D. Conciatori, E. Denarié, H. Sadouki, E. Brühwiler, Chloride penetration model considering the microclimate, in: D.M. Frangopol, E. Brühwiler, M.H. Faber, B. Adey (eds.), Life-Cycle Performance of Deteriorating Structures: Assessment, Design and Management, pp. 68–74, 24–26 March 2003.
[6] D. Conciatori, Effect of microclimate on the corrosion initiation of steel reinforcement in reinforced concrete structures, Doctoral thesis n° 3408, Ecole Polytechnique Fédérale de Lausanne (EPFL), Lausanne, Switzerland, 2005 (in French).
[7] D. Conciatori, E. Brühwiler, Sub-zero transport: low temperature capillary tests in concrete, in: J. Marchand, R. Gagné (Eds.), 2nd International RILEM Symposium, Advances in Concrete through Science and Engineering, Publisher Information, Quebec City, Canada, cds publication, 2006.
[8] E. Denarié, D. Conciatori, E. Brühwiler, Effect of microclimate on chloride penetration into reinforced concrete, in: V.M. Malhotra (Ed.), SP-212 Sixth CANMET/ACI International Conference on Durability of Concrete, Thessaloniki, Greece, 2003.
[9] H. Hamfler, Calculation of temperature, humidity and displacement fields in hardened concrete elements using the finite element method, Deutscher Ausschuss für Stahlbeton (DAfStb) 395 (1988) 159 pp. (in German).
[10] T. Ishida, K. Maekawa, A computational method for performance evaluation of cementitious materials and structures under various environmental actions, Integrated Life-Cycle Design of Materials and Structures — ILCDES2000-, Helsinki, 2000.
[11] C.L. Kamp, P.E. Roelfstra, F.H. Wittmann, Aspects of moisture flow in hardened cement paste and concrete, Report IABSE Colloquium Delft: Computational Mechanics of Concrete Structures — Advances and Applications, 1987, pp. 329–338.
[12] F. Laferrière, Capteur chimique à fibres optiques pour la mesure des ions chlore dans le béton à un stade précoce, Doctoral thesis n° 3322, Ecole Polytechnique Fédérale de Lausanne (EPFL), Lausanne, Switzerland, 2005 (in French).
[13] A. Lindvall, Environmental actions and response, Reinforced Concrete Structures Exposed in Road and Marine Environments, Chalmers University of Technology, Göteborg, 2001.
[14] K. Maekawa, T. Ishida, Service-life evaluation of reinforced concrete under coupled forces and environmental actions, in R. Hooton and al. (eds.), International Conference on Ion and Mass Transport in Cement-Based Materials, Publisher Information, Toronto, Canada, pp. 219–238, 2000.
[15] J. Marchand, E. Samson, D. Burke, P. Tourney, N. Thaulow, S. Sahu, Predicting the Microstructural degradation of concrete in marine environment, in: V.M. Malhotra (Ed.), SP-212 Sixth CANMET/ACI International Conference on Durability of Concrete, Thessaloniki, Greece, 2003.
[16] M. Masi, D. Colella, G. Radaelli, L. Bertolini, Simulation of chloride penetration in cement-based materials, Cement and Concrete Research 27 (10) (1997) 1591–1601.
[17] S.J.H. Meijers, Computational modeling of chloride Ingress in concrete, DUP science, vol. 170, Delft University Press, Delft, Holland, 2003.
[18] N. Oberbeck, H. Duddeck, H. Ahrens, Instationärer Wärme-Feuchte-Schadstoff-Transport in Beton Theorie und Berechnung, Institut für Statik des Technischen Universität Braunschweig, Institut publication, vol. 95–79, 1995, p. 155, Braunschweig, Deutschland.
[19] V.G. Papadakis, M.N. Fardis, C.G. Vayenas, Fundamental concrete carbonation model and application to durability of reinforced concrete, in: J.M. Baker, P.J. Nixon, A.J. Majumdar, H. Davies (Eds.), Proceedings of the Fifth International Conference Durability of Building Materials and Components, Brighton, United Kingdom, 1990, pp. 27–38.
[20] W. Ritthichauy, T. Sugiyama, Y. Tsuji, T. Suda, Thermodynamic law applied for the diffusion of chloride ions in concrete, in: T. Yoshioka, T. Mori, A. Kasuga, T. Miyagawa (Eds.), Proceedings of the First FIB Congress: Concrete Structures in the 21st Century, Osaka, Japan, 2002, pp. 115–120.
[21] G. Roelfstra, R. Hajdin, B. Adey, E. Brühwiler, Condition evolution in bridge management systems and corrosion induced deterioration, ASCE Journal of Bridge Engineering 9 (3) (2004) 268–277.
[22] A.V. Saetta, R.V. Scotta, R.V. Vitaliani, Analysis of chloride diffusion into partially saturated concrete, ACI Materials Journal 90 (5) (1993) 441–451.
[23] E. Samson, J. Marchand, K.A. Snyder, J.J. Beaudoin, Modelling ion and fluid transport in unsaturated cement systems for isothermal conditions, Cement and Concrete Research 35 (2005) 141–153.
[24] Y. Schiegg, H. Böhni, F. Hunkeler, Online-monitoring of corrosion in reinforced concrete structures, FIB, Proceedings of the 1st fib Congress, pp 49–58, Zurich, Switzerland, 2002.
[25] F. Schmidt-Döhl, F.S. Rostasy, A model for the calculation of combined chemical reactions and transport processes and its application to the corrosion of mineral-building materials Part I. Simulation model, Cement and Concrete Research 29 (7) (1999) 1039–1045.
[26] F. Schmidt-Döhl, F.S. Rostasy, A model for the calculation of combined chemical reactions and transport processes and its application to the corrosion of mineral-building materials Part II. Experimental verification, Cement and Concrete Research 29 (7) (1999) 1048–1053.
[27] C.B. Shin, E.K. Kim, Modeling of chloride ion ingress in coastal concrete, Cement and Concrete Research 32 (5) (December 2001) 757–762.
[28] L. Tang, Chloride transport in concrete — Measurements and Prediction, PhD thesis, Building Materials, Chalmers, Göteborg, Sweden, 1996.
[29] O. Truc, J.P. Ollivier, L.-O. Nilsson, Numerical simulation of multi-species transport through saturated concrete during a migration test — MsDiff code, Cement and Concrete Research 30 (10) (2000) 1581–1592.
[30] T. Zhang, E. Samson, J. Marchand, Effect of temperature on ionic transport properties of concrete, Simco Technologies Inc, Quebec, 2005 11 pp., Québec, Canada.